European Heart Journal - Cardiovascular Imaging Advance Access published December 26, 2016

European Heart Journal - Cardiovascular Imaging (2016) **0**, 1–7
doi:10.1093/ehjci/jew215

3D printing of normal and pathologic tricuspid valves from transthoracic 3D echocardiography data sets

Denisa Muraru[1]*, Federico Veronesi[2], Anna Maddalozzo[1], Daniele Dequal[3], Leonardo Frajhof[4], Arnaldo Rabischoffsky[5], Sabino Iliceto[1] and Luigi P. Badano[1]

[1]Department of Cardiac, Thoracic and Vascular Sciences, University of Padua, Padua, Italy; [2]Department of Electrical, Electronic and Information Engineering, University of Bologna, Bologna, Italy; [3]Department of Information Engineering, University of Padua, Padua, Italy; [4]Telemedicine Department, Federal University of the State of Rio de Janeiro, Rio de Janeiro, Brazil; and [5]Hospital Pró-Cardíaco, Rio de Janeiro, Brazil

Received 30 June 2016; accepted after revision 23 September 2016

Aims To explore the feasibility of using transthoracic 3D echocardiography (3DTTE) data to generate 3D patient-specific models of tricuspid valve (TV).

Methods and results Multi-beat 3D data sets of the TV (32 vol/s) were acquired in five subjects with various TV morphologies from the apical approach and analysed offline with custom-made software. Coordinates representing the annulus and the leaflets were imported into MeshLab (Visual Computing Lab ISTICNR) to develop solid models to be converted to stereolithographic file format and 3D print. Measurements of the TV annulus antero-posterior (AP) and medio-lateral (ML) diameters, perimeter (P), and TV tenting height (H) and volume (V) obtained from the 3D echo data set were compared with those performed on the 3D models using a caliper, a syringe and a millimeter tape. Antero-posterior (4.2 ± 0.2 cm vs. 4.2 ± 0 cm), ML (3.7 ± 0.2 cm vs. 3.6 ± 0.1 cm), P (12.6 ± 0.2 cm vs. 12.7 ± 0.1 cm), H (11.2 ± 2.1 mm vs. 10.8 ± 2.1 mm) and V (3.0 ± 0.6 ml vs. 2.8 ± 1.4 ml) were similar ($P =$ NS for all) when measured on the 3D data set and the printed model. The two sets of measurements were highly correlated ($r = 0.991$). The mean absolute error (2D − 3D) for AP, ML, P and tenting H was 0.7 ± 0.3 mm, indicating accuracy of the 3D model of <1 mm.

Conclusion Three-dimensional printing of the TV from 3DTTE data is feasible with highly conserved fidelity. This technique has the potential for rapid integration into clinical practice to assist with decision-making, surgical planning, and teaching.

Keywords 3D printing • three-dimensional • echocardiography • tricuspid annulus • tricuspid regurgitation • tricuspid valve

Introduction

Echocardiography is the key technique to confirm the diagnosis of heart valve disease and to assess its severity and prognosis.[1] However, to properly plan both surgical repair and transcatether intervention on heart valves, we also need a comprehensive morphologic and quantitative assessment of the pathologic anatomy of the valve. Since heart valves are complex three-dimensional (3D) structures, conventional two-dimensional echocardiography (2DE) is often inadequate to provide accurate assessment of the morphology of the diseased heart valves. Nowadays, the rapidly advancing 3D echocardiography (3DE) technology allows us to perform a virtual 'dissection' of the heart *intra vitam* and to obtain unprecedented, realistic views of cardiac valves in just few minutes. By integrating volumetric rendering with motion and flow in real-time, 3DE is the most suited imaging technique for assessing heart valve morphology and function. However, despite the use of the various volume rendering techniques, the display of 3D imaging on flat monitor screens is less than ideal to appreciate the complex geometry of valvular structures.[2]

* Corresponding author. Tel: +39 049 8218640; Fax: +39 049 8211802, E-mail: denisa.muraru@gmail.com

Three-dimensional printing technology has significantly advanced in the past 10 years.[3,4] Three-dimensional printers now have the capability to print at any scale from nearly any type of material.[5] They have been used in various biomedical applications from prosthesis manufacture[3,6–8] to cell and tissue culture.[5,9–11] They have incredible spatial resolution to pick up on microscopic details. There is an emerging field involving the use of 3D simulation data in education[12–14] and preprocedural planning,[15] demonstrating excellent results in general,[8,16] including the cardiology and cardiovascular surgery fields.[15,17–19] Typically, data obtained by cardiac magnetic resonance imaging or computed tomography are used to print high-quality cardiac reconstructions, which may involve intravenous contrast, sedation, and ionizing radiation. There are few reports of 3D printing of transoesophageal echocardiography-based data sets of mitral valves, ventricular septal defects and perivalvular leaks.[18,19] However, transoesophageal echocardiography is uncomfortable for patients and unsuitable for routine assessment of the tricuspid valve (TV) due to its anterior position in the chest. On the other hand, the TV is more challenging to assess with conventional 2DE than mitral valve[20,21] and there is no software package available to perform the quantitative assessment of the complex geometry of this valve which is critical to indicate tricuspid annuloplasty or replacement in patients who are candidates to left-sided valve surgery.[1] Therefore, we explored the feasibility of using transthoracic 3DE data to generate 3D printed patient-specific models of TV and compare measures derived from those models with corresponding measures obtained from the 3DE data sets of the TV.

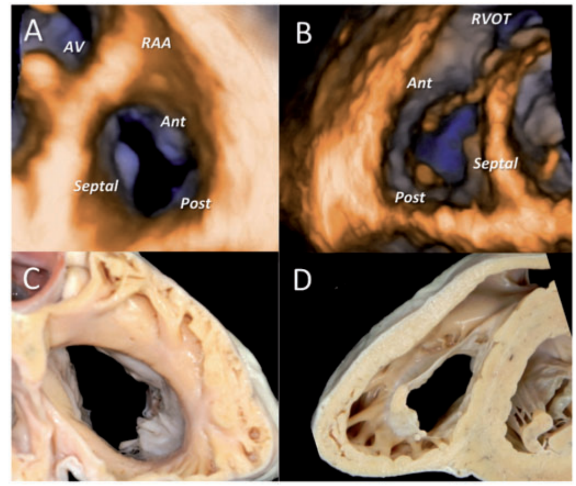

Figure 1 Volume rendering display of a normal TV imaged using transthoracic 3DE shown with the anatomic specimens.
The TV is shown from both the right atrial (obtained after cropping the right atrial roof, panel (*A*) and the right ventricular (obtained after cropping the right ventricle, panel (*B*) perspectives. Corresponding anatomic specimens (courtesy of Prof. Cristina Basso, Cardiovascular Pathology, University of Padua, Italy) are shown in panels (*C* and *D*), respectively.
Ant, anterior tricuspid leaflet; AV, aortic valve; Post, posterior tricuspid leaflet; RAA, right atrial appendage; RVOT, right ventricular outflow tract; Septal, septal tricuspid leaflet. TV, tricuspid valve.

Methods

From our echocardiography database, we selected the 3D data sets of the TV obtained from one healthy volunteer and four patients with tricuspid regurgitation and various morphologies of the TV: functional tricuspid regurgitation with normal tricuspid annulus and leaflet tethering (pulmonary regurgitation in a child with repaired tetralogy of Fallot); functional tricuspid regurgitation with dilated annulus and mild leaflet tethering (paroxysmal atrial fibrillation); functional tricuspid regurgitation with dilated annulus and large leaflet tethering (pulmonary hypertension); organic tricuspid regurgitation with flail of the posterior leaflet. All patients were in sinus rhythm.

Three-dimensional echocardiography

The 3D data sets of the TV were acquired using a commercially available system (Vivid E9, GE Vingmed, Horten, Norway) from the apical approach, with the patient in left lateral decubitus and using a focused right ventricular 4-chamber view. Multi-beat 3D datasets of the TV were acquired by combining six consecutive ECG-triggered sub-volumes in order to obtain high temporal and spatial resolution. Acquisitions were performed during breathhold and by avoiding patient or probe movement in order to obtain data sets free of stitching artefacts. Care was taken to encompass the entire TV in the data sets throughout the cardiac cycle. The selected data sets were cropped and rotated to obtain *en face* views of the TV from both the atrial (Supplementary data online, Video *1*) and ventricular (Supplementary data online, *Video 2*) perspectives in order to visually check the quality of the rendering, absence of artefacts, and dropouts (*Figure 1*).

Image analysis

Then the data sets were imported in a custom-made software package for quantitative assessment of the TV. Initialization started with multi-planar reconstruction to allow the operator to identify the optimal 4-chamber view in combination with the orthogonal longitudinal view. Then, initialization of the tricuspid annulus was manually performed in the mid-systolic frame by marking valve hinge points at end-diastole and end-systole (*Figure 2*). This initialization was performed in eight rotated planes around the TV centre point. Further editing was allowed on any user-identified rotational plane. Input from the user was interactively resampled to 80 points along the annulus using smooth spline interpolation. These 80 points were then automatically tracked throughout the cardiac cycle to obtain the following TA measurements: area (computed as the sum of the triangles composing the 3D mesh connecting all the annulus points), instantaneous area change, perimeter (computed as the sum of the distances between consecutive annulus points), long- and short-axis dimensions and circularity (ratio of short- to long-axis dimensions) (Supplementary data online, *Video 3*). The three commissural points were then manually identified on the 3D looping image with superimposed annulus. Finally an automatic algorithm identified the surface defining the three TV leaflets by means of edge detection (*Figure 2*). Then a surface rendering of the valve was displayed (*Supplementary data online*, *Video 4*). The software package provided automatic measurement of annulus height, area and perimeter, intercommissural distances, tenting height and volume, leaflet areas and angles.

Using specialized segmentation software (MeshLab, Visual Computing Lab ISTICNR), a 3D digital model of the TV was created. The process for creating a printable 3D model from a set of point co-ordinates, known as meshing, is composed of two parts. In the first part, the point cloud is connected with triangles to create a manifold oriented surface. In the second

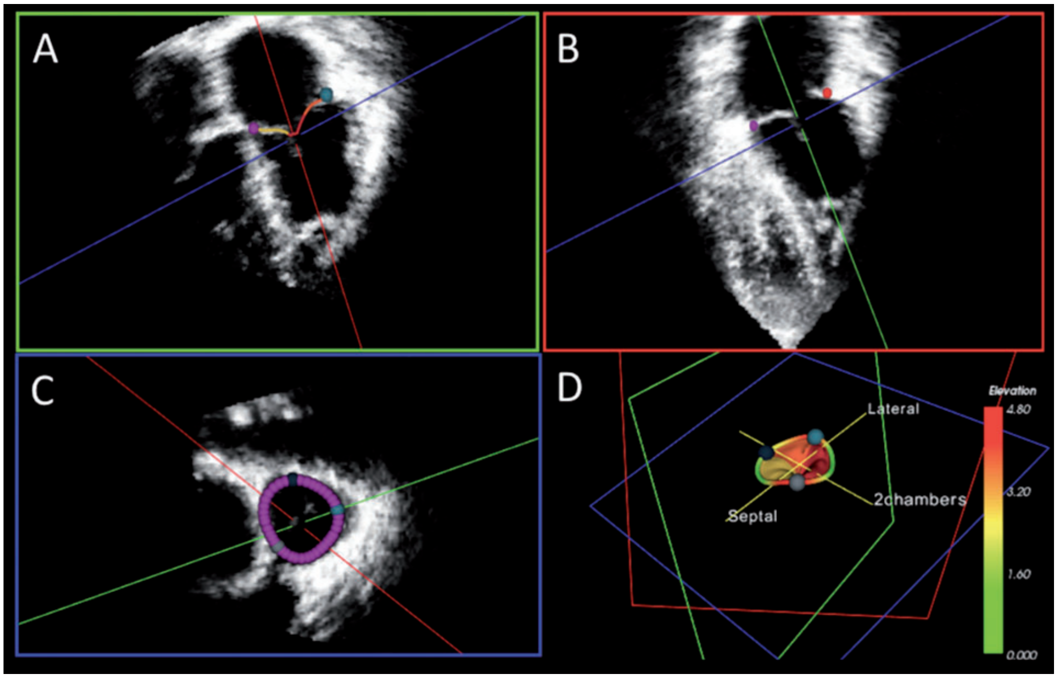

Figure 2 Segmentation of the tricuspid valve by custom software package.
Initially, the optimal four-chamber view (*A*) in combination with the orthogonal two-chamber view (*B*) are identified manually using multi-planar slicing of the 3D data set. The tricuspid annulus is initialized in mid-systole by placing dots (purple points) at the valve hinge points (*panels A* and *B*). This manual initialization is repeated in eight rotated planes around the tricuspid annulus. These points are automatically tracked to obtain measurements of the tricuspid annulus area, perimeter and diameters throughout the cardiac cycle. The three commissural points are then manually identified on the 3D looping image with superimposed annulus (*Panel C*). Finally, an automatic algorithm identifies the surface of the three leaflets by means of edge detection, and a surface-rendering of the tricuspid valve leaflets and annulus is displayed (*Panel D*), allowing quantitative analysis of annulus height, tenting height and volume, leaflet areas and angles, and intercommissural distances. 3D, three-dimensional echocardiography.

part, a fixed thickness is added to the surface, to create the 3D volume. The thickness has been set to 1.5 mm as the best trade-off between robustness and flexibility of the final printed valve. The 3D digital models were exported as stereolithographic files and sent for printing at a 1:1 scale using an EOS FORMIGA P110 (Electro Optical Systems, Munich, Germany) (*Figure 3*).

Measurements of the TV annulus AP and ML[22] diameters, TV tenting height, TV annulus perimeter (P) and TV tenting volume obtained quantitative analysis of the 3DE data sets were compared with those performed directly on the 3D printed models using a caliper (*Figure 4*), a millimeter tape and a syringe (*Figure 5*), respectively.

Statistical analysis

Measurements were tabulated. Absolute error for each measurement was also calculated as the absolute difference of the measurement performed on the 3D echo images and on the printed model, and SEM and standard deviation were derived. A Bland-Altman analysis was performed for assessing the agreement between measurements performed on the 3D echo images and on the printed model.

Results

From December 2010 to July 2014, 3D multi-beat full volume acquisitions of the TV were attempted in 225 healthy volunteers and 423 patients. Feasibility was 95% in healthy volunteers (all of them preselected for good apical acoustic window), and 78% in patients (88% in patients in sinus rhythm and 47% in patients with atrial fibrillation). In patients with sinus rhythm, the main reasons which prevented a successful 3D full-volume acquisition were: frequent ectopic beats (12 patients), limited acoustic window (11 patients), insufficient patient cooperation for breatholding (7 patients), and persistent stitching artefacts despite several acquisition attempts (6 patients).

Among the five subjects whose data sets were selected for testing the feasibility of 3D printing the TV, all five TV were successfully printed (*Figure 6*) and the total time from data set acquisition to final 3D model and stereolithographic file generation was approximately 90 min. The time needed for printing the mesh varies from few minutes to half an hour depending from the complexity of the valve anatomy.

Comparing measurements obtained from slicing the 3D echo data set at the annulus level with those performed directly on the 3D models (*Figure 4*), we found that AP (4.2 ± 0.2 cm vs. 4.2 ± 0 cm; P= NS) and ML (3.7 ± 0.2 cm vs. 3.7 ± 0.1 cm; P= NS) diameters, as well as P (12.6 ± 0.2 vs. 12.7 ± 0.1 cm: P= NS) were similar when measured on the 2D slice and the 3D model. Moreover, the two sets of measurements were highly correlated, (r= 0.991). The mean absolute error (2D − 3D) for AP, ML and P were ≤0.7 ± 0.3 mm, indicating accuracy of the 3D model of <1 mm (*Table 1*).

In addition, other measurements which are clinically useful to plan surgery like TV tenting height (11.2 ± 2.1 mm vs. 10.8 ± 2.1 mm; *P* = NS) and volume (3.0 ± 0.6 ml vs. 2.8 ± 1.4 ml; *P* = NS) could also be performed directly on the model obtaining values which are similar to those measured on the 3D echo data sets (*Figures 4* and *5*) (*Table1*).

Finally, linear and perimeter measurements performed on the 3D physical model were highly reproducible with intra- and inter-observer variability 0.5 ± 1 mm and 0.8 ± 1 mm, respectively.

Discussion

This is the first study to report on the feasibility and the accuracy of 3D printed models of the TV obtained from 3DE data sets acquired using the transthoracic approach. The main results of our study can be summarized as: (i) transthoracic acquisition of 3DE data sets of the TV is highly feasible in both normal subjects and patients; (ii) three-dimensional printed physical models of the TV can be effectively and quickly obtained from transthoracic 3DE data sets; (iii) linear and volume measurements performed on 3D printed TV models are similar to those obtained from the volume-rendered images and are

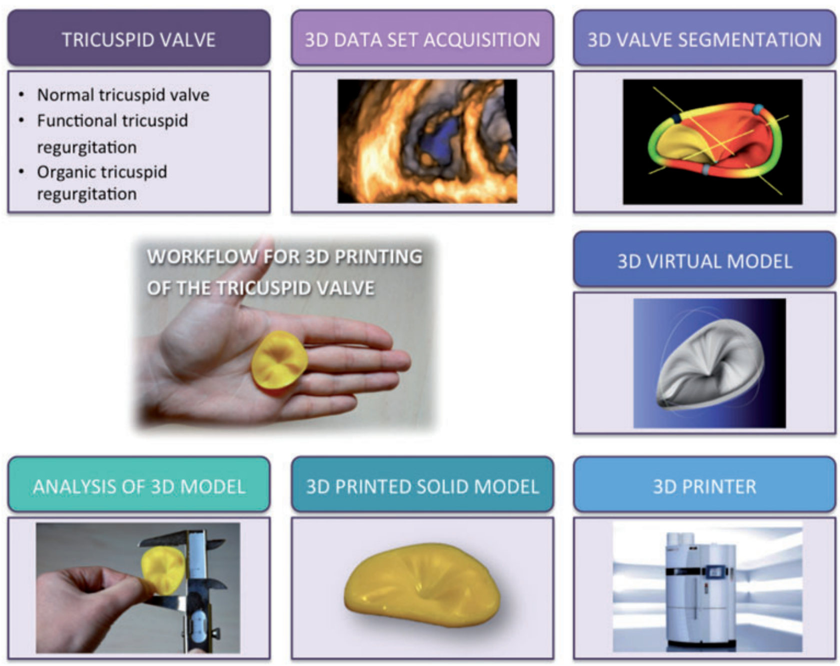

Figure 3 Workflow associated with printing a 3D solid model of the tricuspid valve.
A sample of workflow is shown diagrammatically from the transthoracic acquisition of the 3DE data set, to its segmentation, creation of a virtual 3D model and stereolithographic file that can be printed using any commercially available 3D printer. The 3D solid model of the valve can be used to appreciate valve morphology and perform qualitative and quantitative analysis useful for pre-procedural (surgical or interventional) planning and teaching. 3D, three-dimensional.

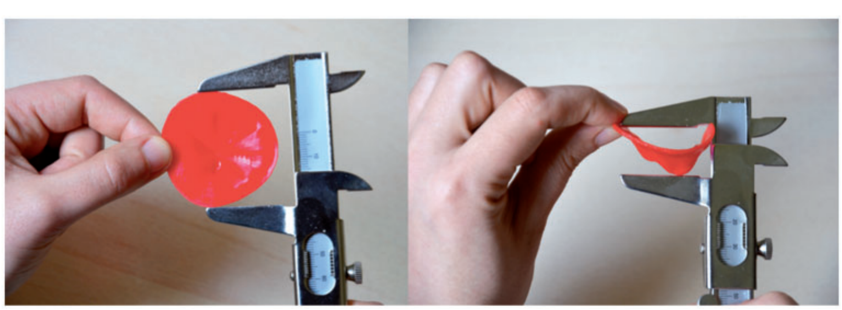

Figure 4 Measurement of tricuspid valve annulus diameter (left panel) and tenting height (right panel) on the 3D printed model using a caliper.

easy to perform; (iv) 3D printed models allow to better appreciate TV 3D shape and leaflet morphology compared to virtual rendered models.

In asymptomatic patients with less than severe tricuspid regurgitation undergoing cardiac surgery for left-sided valvular lesions, indications to tricuspid annuloplasty/valve replacement are controversial (the level of evidence is only C) and based on the measurement of tricuspid annulus diameter in apical 4-chamber view using 2DE. However, a single linear measurement taken from a single 2DE apical view has been shown to be poorly reproducible and unlikely to describe the dynamic, complex 3D geometry of the TV. Moreover, innovative TV interventions require an advanced understanding of spatial relationships among the components of TV apparatus.[23–25] Finally, in the last few years there has been a dramatic increase of investigative catheter-based therapies for tricuspid functional regurgitation that involve both modification of tricuspid apparatus structures and implantation of novel devices.[26] Despite the technical advancements and the incremental clinical use of 3DE that has definitely improved our understanding of pathophysiology and functional anatomy of the regurgitant TV,[20,21,27] the effectiveness of displaying 3D data sets as projections on 2D flat panels has been questioned.[2] Three-dimensional printing of the TV has the potential to allow us to move a step forward in understanding and quantifying tricuspid annulus geometry, elevating our impressions from textured flat-panel coloured perspectives to actual exploration of the complex geometry of the TV, with the potential to guide personalized care of patients with functional and organic tricuspid regurgitation.[28]

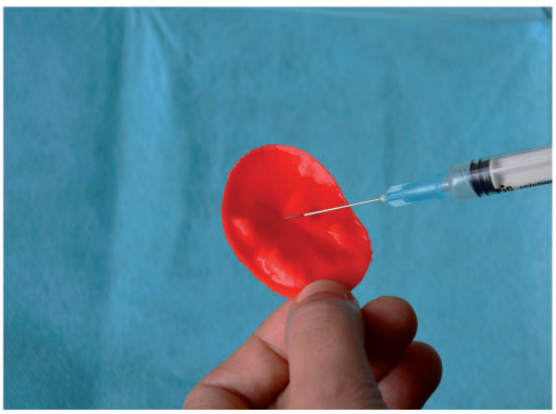

Figure 5 Measurement of the tricuspid valve tenting volume using the 3D printed model filled with water and a syringe.

Our data show that despite the TV is difficult to image using 3D transesophageal echocardiography, cardiac magnetic resonance and computerized tomography due to its position in the chest, its spatial orientation and the thin leaflets, acquisition of 3D full volume data sets of the TV from the transthoracic approach with a good spatial and a reasonable temporal resolution was quite feasible. Our results have been confirmed by others[29,30] and are quite encouraging for the systematic application of 3D transthoracic echocardiography to assess the TV in the clinical routine of the echocardiography laboratory.

Despite over the past few years both clinical cardiologists and cardiac surgeons have become more and more aware of the morbidity and mortality related to the presence of functional tricuspid regurgitation in patients with successful surgery of left heart valve surgery,

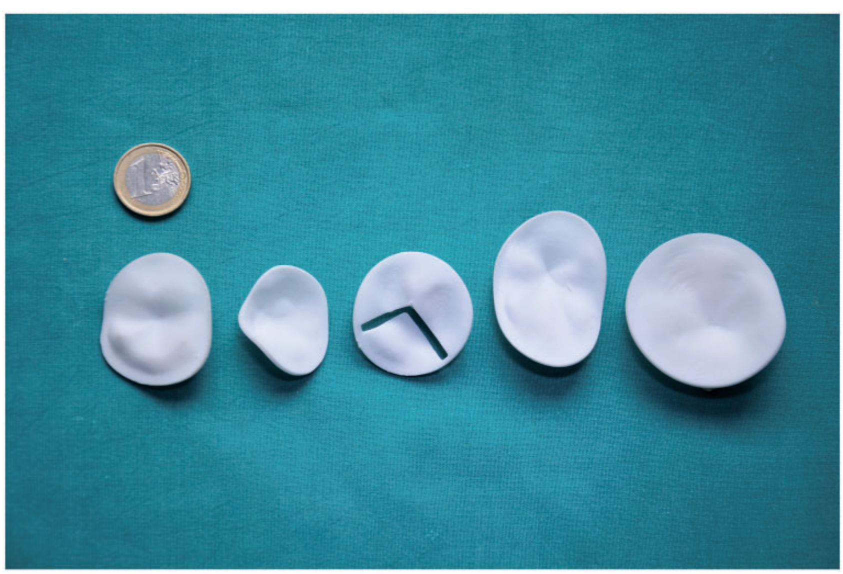

Figure 6 Three-dimensional printed models of five subjects with various conditions and tricuspid valve morphologies.
From the left to right: normal tricuspid valve; functional tricuspid regurgitation with leaflet tethering and normal annulus size (child with repaired tetralogy of Fallot); organic post-traumatic tricuspid regurgitation with flail of the posterior leaflet; functional tricuspid regurgitation with dilated annulus and mild leaflet tethering (paroxysmal atrial fibrillation); functional tricuspid regurgitation with severely dilated annulus and large leaflet tethering (pulmonary arterial hypertension). A 1 Euro coin is shown for an easier appreciation of the actual size of the valves.

Table 1 Comparison of measurements describing TV geometry performed on the 3D data set using the custom made software and directly on the 3D printed model using a caliper, a millimeter tape and a syringe, respectively

	Tricuspid annulus antero-posterior diameter (mm)			Tricuspid annulus medio-lateral diameter (mm)			Tricuspid annulus perimeter (mm)			TV leaflet tenting height(mm)			TV tenting volume(ml)		
Patient	3D DS	3D PR	Δ	3D DS	3D PR	Δ	3D DS	3D PR	Δ	3D DS	3D PR	Δ	3D DS	3D PR	Δ
1	40.2	39.0	1.2	33.8	35.0	1.2	119.0	120.0	1.0	6	6	0	1	1	0
2	48.7	48.0	0.7	48.0	48	0	155.7	157.0	1.3	16	15	1	5	4	1
3	49.0	49.0	0.0	34.0	34.0	0	135.3	137.0	1.7	13	13	0	3	3.5	0.5
4	34.0	35.0	1.0	32.0	30.0	2	100.6	101.0	0.4	9	9	0	2	3	1
5	38.1	38.5	0.4	36.4	36.5	0.1	116.9	118.0	1.1	NA	NA	NA	NA	NA	NA

3D, three-dimensional; Δ, absolute difference; DS, data set; NA, not applicable (TV flail); PR, printed model; TV, tricuspid valve.

indications for tricuspid annuloplasty in such patients are based on elusive evidences (class C)[1] and, differently from the mitral and aortic valves, software packages allowing quantitative assessment of 3D data sets of the TV are lacking.

The possibility to obtain a 3D printed TV from a 3DE data set and to both directly visualize the morphological changes occurred in the diseased valve and measure the parameters needed for surgical planning have great potential to help to identify patient-specific reparative strategies, particularly in complex or congenital TV abnormalities. 3D printing could be useful to design new transcatheter devices to help those patients who are judged to be at high surgical risk. Among the novel percutaneous procedures for TV repair that are currently being tested,[26] the transcatheter annuloplasty techniques may derive a particular benefit from the application of 3D printing to obtain patient-specific measurements of TV annular perimeter and non-planar area, as well as to quantitate leaflet tenting volume and post-procedural changes on leaflet geometry and coaptation as a consequence from annulus shrinking. This is of utmost importance, since not all patients with annulus dilation may be optimally treated by restrictive annuloplasty procedures only.[23] Thus, 3D printing could become a useful adjunct for identifying those patients with the most suitable TV anatomy (i.e. predominant annulus dilation and absent/minor leaflet tethering) for this type of procedure.

The possibility to reproduce 3D printed copies of cardiac anatomic specimens from ultrasound data will allow a routine use of 3D printing technology in medical education. 3D printed reproductions of cardiac structures are durable and reasonably unexpensive, relatively easy to reproduce in multiple copies, and 3D non-invasive imaging capabilities are cost-effective and widely available nowadays. Thus, 3D printing appears promising as an attractive alternative or adjunct in medical teaching for universities with limited/no access to cadavers for teaching purposes due to financial or logistical reasons, and social or cultural barriers in some countries. Finally, 3D printing may be useful to study flow-related physiology and to replicate pathologic haemodynamic conditions for a more in-depth understanding of valvular dysfunction, albeit this application is limited at present by lack of tissue-specific materials.[31] 3D printing of the TV using material which physical characteristics resemble biological tissues may fasten the development of patient-specific devices and reduce the cost of their development.

In our study, we were able to reproduce static models of the TV annulus and leaflets at mid-systole using a custom-made prototype software. Although this software could be theoretically adapted also for obtaining 3D models of mitral or aortic annuli, several software packages for mitral and aortic valve analysis by 3DE are already commercially available, allowing to obtain valve-specific modelling and meshes that can be used for 3D printing.[19] Since valves are highly dynamic structures during the cardiac cycle, one may question the reliability of planning surgical repairs based on a static model of the valve. Ideally, a printed model would be able to somehow mimic the anatomic and potentially physiologic changes that occur during the cardiac cycle. However, surgical indications have been based so far on questionable linear measurements of TV annulus taken on a single two-dimensional view at end-diastole. In addition, some preliminary data have shown the possibility to use special material that can resemble the physiological characteristics of the biological tissue when the structure is inserted in a pulsatile flow imaging circuit.[31]

Study limitations

The number of 3D printed valves in our study was small and we did not test the accuracy of our measurements against any gold standard. However, a real gold standard for tricuspid annulus and valve geometry measurements is difficult to find since intraoperative measurements are highly variable depending on the traction performed by the surgeon on the annulus,[32] and cardiac magnetic resonance and computerized tomography provide only tomographic slices to be measured not truly representing the complex 3D geometry of the TV.

We have obtained 3D prints of TV annulus and leaflets using monochrome 3D printing technology from surface-rendered models obtained by prototype software. Therefore, our 3D printed models of TV did not allow to reproduce fine anatomical details of the valve, such as the exact localization and the distance between commissures. Our models also did not include other components of TV apparatus (such as chordae, papillary muscles), nor displayed spatial relationships with right heart structures (caval veins, right atrium, right ventricle, right coronary artery etc) that can be more readily obtained with other imaging modalities, such as 3D angio CT.[26] With the current 3D ultrasound and printing technology, thin mobile structures, such as valves and the subvalvar apparatus, remain challenging to recreate. For more realistic 3D prints of the heart from 3D echo data (capable of replicating all the relevant anatomic structures included in the data set), we would need dedicated algorithms able to automatically extract 3D coordinates of cardiac structures from routine 3D echocardiographic data sets and enable structure-specific colour maps. Finally, having software solutions able to convert 3D meshes into printable files implemented on board on the future 3D ultrasound systems would allow an easier and faster integration of 3D printing for clinical and research purposes.

Conclusions

Three-dimensional printing of the TV from 3D data sets obtained using echocardiography and transthoracic approach is feasible with highly conserved fidelity. Printing solid 3D models of TV allows morphological and quantitative analysis of valve geometry. The availability of 3D ultrasound systems equipped with dedicated software on board able to extract the 3D coordinates of cardiac structures and convert ultrasound data into 3D printable file formats would allow an easier and faster integration of 3D printing for clinical and research purposes. Thus, 3D printing has a great potential for integration into clinical practice to assist with decision-making, surgical or interventional planning and medical teaching.

Conflict of interest: None declared.

References

1. Vahanian A, Alfieri O, Andreotti F, Antunes MJ, Baron-Esquivias G. *et al*. Guidelines on the management of valvular heart disease (Version 2012). *Eur Heart J* 2012;**33**:2451–96.
2. Farooqi KM, Sengupta PP. Echocardiography and three-dimensional printing: sound ideas to touch a heart. *J Am Soc Echocardiogr* 2015;**28**:398–403.
3. Marro A, Bandukwala T, Mak W. Three-dimensional printing and medical imaging: a review of the methods and applications. *Curr Probl Diagn Radiol* 2016;**45**:2–9.
4. Kim MS, Hansgen AR, Wink O, Quaife RA, Carroll JD. Rapid prototyping: a new tool in understanding and treating structural heart disease. *Circulation* 2008;**117**:2388–94.
5. Chia HN, Wu BM. Recent advances in 3D printing of biomaterials. *J Biol Eng* 2015;**9**:4.
6. Yun PY. The application of three-dimensional printing techniques in the fi eld of oral and maxillofacial surgery. *J Korean Assoc Oral Maxillofac Surg* 2015;**41**:169–70.
7. Malik HH, Darwood AR, Shaunak S, Kulatilake P, El-Hilly AA, Mulki O. *et al*. Three-dimensional printing in surgery: a review of current surgical applications. *J Surg Res* 2015;**199**:512–22.
8. AlAli AB, Griffin MF, Butler PE. Three-dimensional printing surgical applications. *Eplasty* 2015;**15**:e37.
9. Hsieh FY, Lin HH, Hsu SH. 3D bioprinting of neural stem cell-laden thermoresponsive biodegradable polyurethane hydrogel and potential in central nervous system repair. *Biomaterials* 2015;**71**:48–57.
10. Collins SF. Bioprinting is changing regenerative medicine forever. *Stem Cells Dev* 2014;**23(Suppl 1)**:79–82.
11. Murphy SV, Atala A. 3D bioprinting of tissues and organs. *Nat Biotechnol* 2014;**32**:773–85.
12. Liew Y, Beveridge E, Demetriades AK, Hughes MA. 3D printing of patient-specific anatomy: a tool to improve patient consent and enhance imaging interpretation by trainees. *Br J Neurosurg* 2015;**29**:712–4.
13. Mahmoud A, Bennett M. Introducing 3-dimensional printing of a human anatomic pathology specimen: potential benefits for undergraduate and postgraduate education and anatomic pathology practice. *Arch Pathol Lab Med* 2015;**139**:1048–51.
14. Bernhard JC, Isotani S, Matsugasumi T, Duddalwar V, Hung AJ, Suer E. *et al*. Personalized 3D printed model of kidney and tumor anatomy: a useful tool for patient education. *World J Urol* 2016;**34**:337–45.
15. Farooqi KM, Saeed O, Zaidi A, Sanz J, Nielsen JC, Hsu DT. *et al*. 3D printing to guide ventricular assist device placement in adults with congenital heart disease and heart failure. *JACC Heart Fail* 2016;**4**:301–11.
16. Dickinson KJ, Matsumoto J, Cassivi SD, Reinersman JM, Fletcher JG, Morris J. *et al*. Individualizing management of complex esophageal pathology using three-dimensional printed models. *Ann Thorac Surg* 2015;**100**:692–7.
17. Costello JP, Olivieri LJ, Su L, Alfares F, Thabit O, Marshall MB. *et al*. Incorporating three-dimensional printing into a simulation-based congenital heart disease and critical care training curriculum for resident physicians. *Congenit Heart Dis* 2015;**10**:185–90.
18. Olivieri LJ, Krieger A, Loke YH, Nath DS, Kim PC, Sable CA. Three-dimensional printing of intracardiac defects from three-dimensional echocardiographic images: feasibility and relative accuracy. *J Am Soc Echocardiogr* 2015;**28**:392–7.
19. Mahmood F, Owais K, Taylor C, Montealegre-Gallegos M, Matyal R, Panzica P. *et al*. Three-dimensional printing of mitral valve using echocardiographic data. *JACC Cardiovasc Imaging* 2015;**8**:227–9.
20. Muraru D, Badano LP, Sarais C, Solda E, Iliceto S. Evaluation of tricuspid valve morphology and function by transthoracic three-dimensional echocardiography. *Curr Cardiol Rep* 2011;**13**:242–9.
21. Badano LP, Agricola E, Perez de Isla L, Gianfagna P, Zamorano JL. Evaluation of the tricuspid valve morphology and function by transthoracic real-time three-dimensional echocardiography. *Eur J Echocardiogr* 2009;**10**: 477–84.
22. Boudjemline Y, Agnoletti G, Bonnet D, Behr L, Borenstein N, Sidi D. *et al*. Steps toward the percutaneous replacement of atrioventricular valves an experimental study. *J Am Coll Cardiol* 2005;**46**:360–365.
23. Dreyfus GD, Martin RP, Chan KM, Dulguerov F, Alexandrescu C. Functional tricuspid regurgitation: a need to revise our understanding. *J Am Coll Cardiol* 2015;**65**:2331–6.
24. Rodes-Cabau J, Taramasso M, O'Gara PT. Diagnosis and treatment of tricuspid valve disease: current and future perspectives. *Lancet* 2016 [Epub ahead of print]. doi:10.1016/S0140-6736(16)00740-6.
25. O'Neill WW, O'Neill BP. Transcatheter tricuspid valve intervention: the next frontier. *J Am Coll Cardiol* 2015;**65**:1196–8.
26. Taramasso M, Pozzoli A, Guidotti A, Nietlispach F, Inderbitzin DT, Benussi S. *et al*. Percutaneous tricuspid valve therapies: the new frontier. *Eur Heart J* 2016 [Epub ahead of print]. doi:10.1093/eurheartj/ehv766.
27. Muraru D, Surkova E, Badano LP. Revisit of functional tricuspid regurgitation. Current trends in the diagnosis and management. *Korean Circ J* 2016:**46**: 443–55
28. O'Neill B, Wang DD, Pantelic M, Song T, Guerrero M, Greenbaum A. *et al*. Transcatheter caval valve implantation using multimodality imaging: roles of TEE, CT, and 3D printing. *JACC Cardiovasc Imaging* 2015;**8**:221–5.
29. Anwar AM, Geleijnse ML, Soliman OI, McGhie JS, Frowjin R, Nemes A. *et al*. Assessment of normal tricuspid valve anatomy in adults by real-time three-dimensional echocardiography. *Int J Cardiovasc Imaging* 2007;**23**:717–24.
30. Addetia K, Yamat M, Mediratta A, Medvedofsky D, Patel M, Ferrara P. *et al*. Comprehensive two-dimensional interrogation of the tricuspid valve using knowledge derived from three-dimensional echocardiography. *J Am Soc Echocardiogr* 2016;**29**:74–82.
31. Maragiannis D, Jackson MS, Igo SR, Schutt RG, Connell P, Grande-Allen J. *et al*. Replicating patient-specific severe aortic valve stenosis with functional 3D modeling. *Circ Cardiovasc Imaging* 2015;**8**:e003626.
32. Dreyfus J, Durand-Viel G, Raffoul R, Alkhoder S, Hvass U, Radu C. *et al*. Comparison of 2-Dimensional, 3-Dimensional, and surgical measurements of the tricuspid annulus size: clinical implications. *Circ Cardiovasc Imaging* 2015;**8**: e003241.